Wireless Power Transfer, 2019, 6(1), 57–66.
doi:10.1017/wpt.2019.3

RESEARCH ARTICLE

RF-DC conversion efficiency improvement for microwave transmission with pulse modulation

TAKASHI HIRAKAWA, CE WANG AND NAOKI SHINOHARA

Microwave power transfer (MPT) can solve certain types of problems. For example, Internet of Things requires a flexible configuration of sensor networks, which is hindered by wired-charging sensors. This problem can be overcome by MPT techniques. However, the transmission efficiency of MPT is lower than that of wired transmission. This study focuses on the operation of rectifiers having a pulse-modulated input signal. Although a pulse-modulated wave is effective for improving the RF-DC conversion efficiency, the output voltage waves of rectifiers have a high ripple content. Moreover, the harmonic balance method cannot be used to simulate the operation of a pulse-modulated rectifier. To reduce the ripple content, a smoothing capacitor should be connected in parallel to an output load. We investigated the influence of a smoothing capacitor, the general characteristics of rectifiers under pulse-modulated waves, and the effectiveness of using pulse-modulated waves for improving RF-DC conversion efficiency. In conclusion, we reveal a necessary condition of the smoothing capacitor for improvement, demonstrate the effectiveness of pulse modulation, and show that the optimum impedance with a pulse-modulated wave input is an inverse of duty ratio times as compared to that with continuous wave input.

Keywords: Rectifier, Pulse modulation, RF-DC conversion efficiency, High PAPR

Received 3 September 2018; Revised 9 February 2019; Accepted 12 February 2019; first published online 26 March 2019

I. INTRODUCTION

Microwave power transfer (MPT) can provide solutions to some critical problems. Currently, the necessity of the Internet of Things (IoT) technique is increasing. IoT requires a flexible configuration of sensor networks, which is hindered by wired-charging sensors and MPT can be the solution. MPT techniques have been improved [1, 2]; however, there are some shortcomings, namely the lack of interference with communication and low transmitting efficiency, which will be the focus of our study. MPT requires rectifiers for the RF-DC conversion. Information and power transmission can be operated at the same frequency using pulse-modulated waves [3]. On the other hand, simultaneous wireless information and power transmission using pulse modulation has been considered in some research [4, 5]. Since pulse-modulated waves are compatible with the MPT system of communication, we have used it herein (Fig. 1) [6]. The modeling, simulation, and analytical calculation methods have been discussed previously [7–9]. In addition, the general characteristics of rectifiers have been studied [10, 11]. Figure 2 shows the general characteristics of the RF-DC conversion efficiency [11]. The use of signals with a high peak-to-average power ratio (PAPR) improves the RF-DC conversion efficiency [12]. The efficiency decreases with a low input voltage, and a small voltage applied to the diode is adversely affected by the threshold voltage (Fig. 2). In contrast, with a high input, the voltage applied to the diode exceeds the breakdown voltage, and the RF-DC conversion efficiency decreases. Herein, the RF-DC conversion efficiency is improved using the low input voltage. Figure 3 shows the comparison between the output voltage under continuous wave (CW) and intermittent CW (ICW) inputs displaying the increasing voltage of rectifiers under the input with a high PAPR. The application of chaotic waves [13], ultra-wide bandwidth signals [14], multisine waves [15], or modulated waves [16] can improve the RF-DC conversion efficiency because these waves have a high PAPR, similar to the pulse-modulated waves. Thus, pulse modulation is effective at improving the RF-DC conversion efficiency of rectifiers and solving other problems. Some studies are focusing on a pulse-modulated wave as we mentioned above [4, 5]. These research papers focused on information transmission by amplitude shift keying and discussed about the output voltage wave for simultaneous wireless information and power transmission (SWIPT). Their research shows pulse modulation is at least effective for SWIPT. This research discusses operation in more detail and focuses on improving RF-DC conversion efficiency of rectifiers. A pulse-modulated wave has two fundamental frequencies, repetition and carrier frequencies. The harmonic balance method is of no use for analyzing the operation under pulse-modulated waves. To analyze the operation

Kyoto University, Gokasho, Uji-shi, Kyoto-fu, 551-0011, Japan
Corresponding author:
Takashi Hirakawa
Email: takashi_hirakawa@rish.kyoto-u.ac.jp

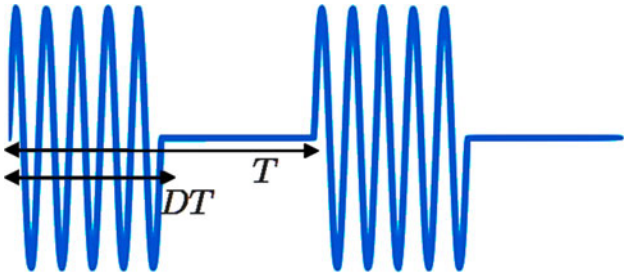

Fig. 1. Waveform of pulse-modulated waves.

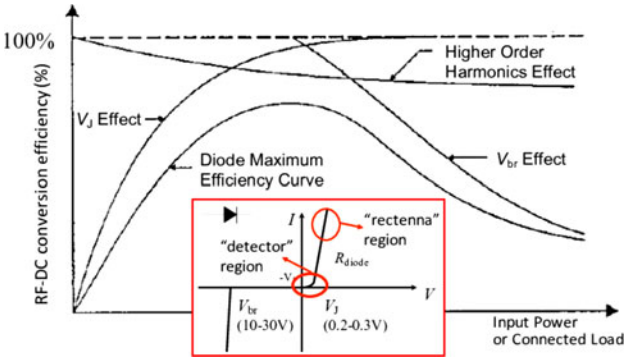

Fig. 2. Theoretical characteristics of the RF-DC conversion efficiency [2].

of the rectifiers under pulse-modulated waves, one needs to employ the transient method since the analysis using the harmonic balance method is difficult. In this study, the operation of single-shunt rectifiers (Fig. 4) under pulse-modulated input is studied. The operation of rectifiers with pulse-modulated input was discussed previously [17]. However, this work did not discuss thoroughly enough the details regarding the circuit design method and the conditions for using pulse-modulated waves. We focus on the effects of smoothing capacitance and of the parameters of the pulse modulations in this research. In addition, the effectiveness of pulse modulation for improvement and rectifier operations is discussed in detail. Our study analyzes a general operation of rectifiers with pulse-modulated waves and shows the effectiveness of the pulse modulation for improving the RF-DC conversion efficiency by theory, simulations, and experiments. In addition, we suggest an analytical approach for rectifiers to design pulse-modulated waves which have low repetition frequency.

II. THEORETICAL ANALYSIS OF THE RECTIFIER OPERATION UNDER PULSE-MODULATED INPUT

A pulse-modulated wave rectifier that utilizes the charging and discharging of a smoothing capacitor significantly impacts V_{out}. This section discusses the operation of rectifiers as affected by a smoothing capacitor and considers the operation of the rectifiers under pulse modulation.

A) Parameters used in this paper

Table 1 shows the definition of the variables used herein. The following equations are used to express the relations among these variables:

$$P_{input} = DP_{RF} \tag{1}$$

$$P_{output} = \frac{1}{T}\int_0^T \frac{V_{out}(t)^2}{R_{load}}dt \tag{2}$$

$$P_{DC} = \frac{V_{DC}^2}{R_{load}} \tag{3}$$

$$V_{DC} = \frac{1}{T}\int_0^T V_{out}(t)dt \tag{4}$$

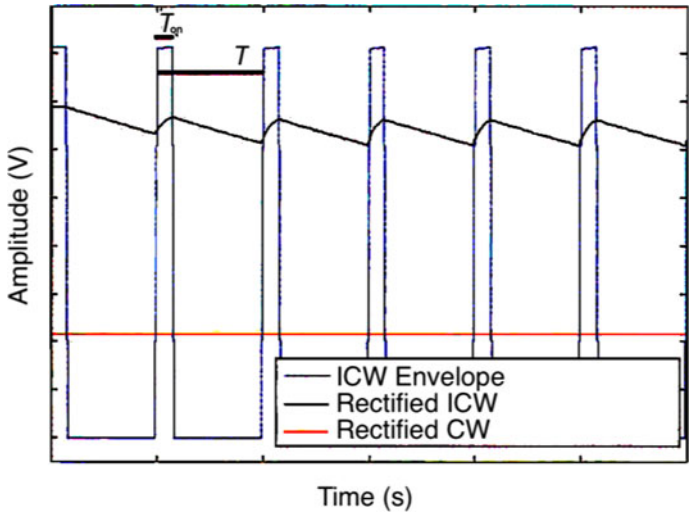

Fig. 3. Comparison between the output voltage using the CW and ICW inputs [12].

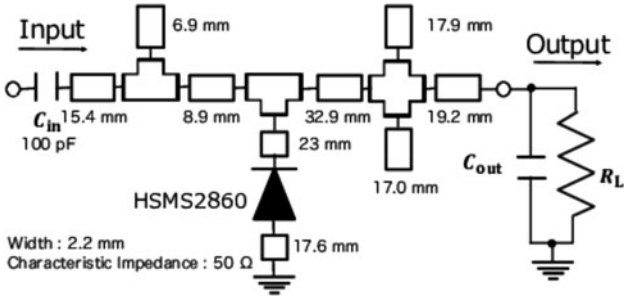

Fig. 4. Schematic of single-shunt rectifiers.

$$\eta_{DC} = \frac{P_{DC}}{P_{input}} \tag{5}$$

$$\eta_{out} = \frac{P_{output}}{P_{input}} \tag{6}$$

$$M = \frac{\max\left(V_{out}(t)\right) - \min\left(V_{out}(t)\right)}{V_{DC}} \tag{7}$$

B) Discussion on the fluctuation of V_{out}

The fluctuation of V_{out} is caused by the charging and discharging of the smoothing capacitor. The amount of electric charge stored during charging is designated as Q. In the steady state, the amount of electrical charge stored during the charging period is same as that flowing out from C_{out} during the discharging period. Hence, equation (8) is obtained:

$$\begin{aligned} Q &= C_{out}(V_{out}(t_o + DT) - V_{out}(t_o)) \\ &= \int_{t_o+DT}^{t_o+T} \frac{V_{out}(t)}{R_L} dt. \end{aligned} \tag{8}$$

Table 1. Definition of variables.

Variables	Definition
P_{RF}	Power of a carrier wave (W)
P_{input}	Average of input power (W)
P_{output}	Average of output power (W)
P_{DC}	DC power of output (W)
$V_{out}(t)$	Output voltage of rectifiers (V)
V_{DC}	DC component of $V_{out}(t)$ (V)
C_{in}	Capacitance of input capacitor (fixed as 100 pF)
C_{out}	Capacitance of smoothing capacitor (F)
R_{load}	Load resistance (Ω)
η_{RF}	RF-DC conversion efficiency with CW drive condition
η_{DC}	RF-DC conversion efficiency
η_{out}	P_{input} to P_{output} ratio
f_r	Repetition frequency (Hz)
T	Repetition period (s)
M	Ripple content of $V_{out}(t)$
D	Duty ratio of pulse modulation

In contrast, equation (9) is obtained:

$$\int_{t_o+DT}^{t_o+T} \frac{V_{out}(t)}{R_L} dt \le \frac{\max\left(V_{out}\right)}{R_L}(1-D)T. \tag{9}$$

Therefore, the maximum value of the voltage change is expressed using equation (10):

$$\max(V_{out}) - \min\left(V_{out}\right) \le \frac{\max(V_{out})}{C_{out}R_L}(1-D)T. \tag{10}$$

Equation (11) is derived from equation (10):

$$\frac{\min(V_{out})}{\max(V_{out})} \ge 1 - \frac{(1-D)T}{C_{out}R_L}. \tag{11}$$

Consequently, equation (12) is derived as a condition wherein a sufficiently small fluctuation occurs:

$$C_{out} \gg \frac{1-D}{R_L f_r}. \tag{12}$$

The operation of rectifiers with the condition satisfying equation (12) is discussed in the next subsection. With the condition equation (12) unsatisfied, the output voltage wave is in the steady state, as shown in Fig. 5. The waveform consists of two functions, f_{rising} and $f_{falling}$. Figure 6 shows the forms of their functions. E means the DC voltage in the steady state with CW input, which has P_{RF} input power. $E_{\max}$ and $E_{\min}$ respectively indicate the maximum and minimum voltages of an output wave under pulse-modulated input. Herein, the change in V_{out} during charging is denoted as $f_{rising}(t)$ and that during discharging as $f_{falling}(t)$. $f_{rising}(t)$ and $f_{falling}(t)$ satisfy equations (13) and (14), respectively:

$$\begin{aligned} &f_{rising}(DT + t_{ro}) - f_{rising}(t_{ro}) \\ &\quad = f_{falling}((1-D)T + t_{fo}) - f_{falling}(t_{fo}), \end{aligned} \tag{13}$$

$$f_{falling}(t_{fo}) = f_{rising}(DT + t_{ro}). \tag{14}$$

These are the boundary conditions of a steady state. When we know the transient operations of rectifiers during charging and discharging, the operations of rectifiers under the pulse-

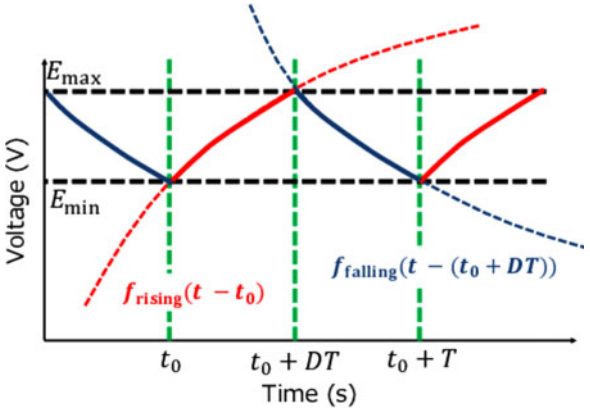

Fig. 5. V_{out} with pulse-modulated waves in the steady state.

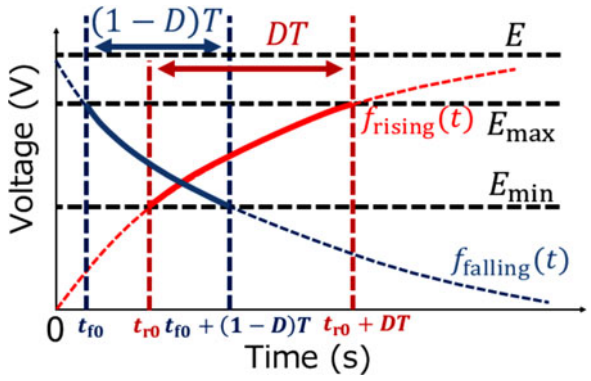

Fig. 6. Definition of $f_{rising}(t)$ and $f_{falling}(t)$.

modulated waves can be calculated by equations (13) and (14). Figures 7 and 8 show the equivalent circuits at the rising and falling edges. $f_{rising}(t)$ and $f_{falling}(t)$ can be determined by the easy calculations shown below:

$$f_{rising}(t) = E\left(1 - \exp\left(-\frac{t}{\tau_{rising}}\right)\right), \tag{15}$$

$$f_{falling}(t) = E\exp\left(-\frac{t}{\tau_{falling}}\right). \tag{16}$$

When the C_{in} and junction capacitance of the diode are small, $\tau_{falling}$ is equal to $C_{out}R_{load}$. In addition, equation (16) has been discussed and used in some papers [4, 5]. The rise operation is complex for the microwave propagation; therefore, τ_{rise} cannot be obtained from a theoretical analysis.

C) Analysis of the rectifier with a sufficiently large smoothing capacitor

This subsection discusses the rectifier operation under the conditions of equation (12). The current is defined as shown in Fig. 9. We let the average of I and V_{out} be represented as $\bar{I}$ and $\overline{V_{out}}$. In addition, the average current flowing through the capacitor during charging is a times as large as $\bar{I}$. When the fluctuation of V_{out} is sufficiently small, the fluctuation of I is also very small. Equation (17) is obtained by considering the conservation of charge during the charging and

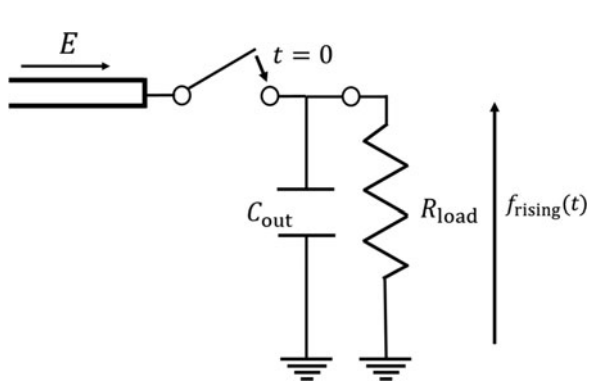

Fig. 7. Equivalent circuit at the rising edge.

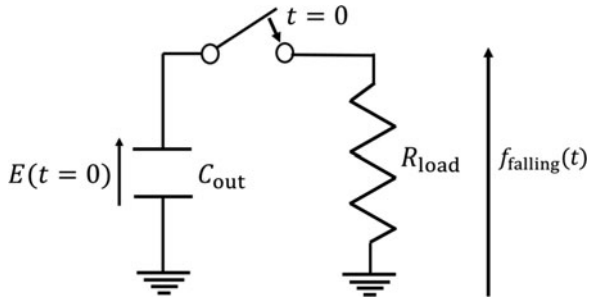

Fig. 8. Equivalent circuit at the falling edge.

discharging of a steady state capacitor:

$$a\bar{I}D = (1 - D)\bar{I}. \tag{17}$$

With a sufficiently small voltage fluctuation, the apparent impedance also has a sufficiently small change. Let R be the resistance observed from the rectifier circuit during charging as expressed in equation (18):

$$R = \frac{\overline{V_{out}}}{(a+1)\bar{I}}. \tag{18}$$

R_{load} is represented by equation (19):

$$R_{load} = \frac{\overline{V_{out}}}{\bar{I}}. \tag{19}$$

Equation (20) is derived using equations (17)–(19):

$$R = DR_{load}. \tag{20}$$

Equation (20) shows that the rectifier operates under the conditions of input power P_{input} and load resistance DR_L during charging. Using η_{RF} with P_{input} of input power and DR_L of load resistance, we obtain equation (21):

$$\overline{V_{out}} = \sqrt{\frac{\eta_{RF}P_{input}R}{D}} = \sqrt{\eta_{RF}P_{input}R_{load}}. \tag{21}$$

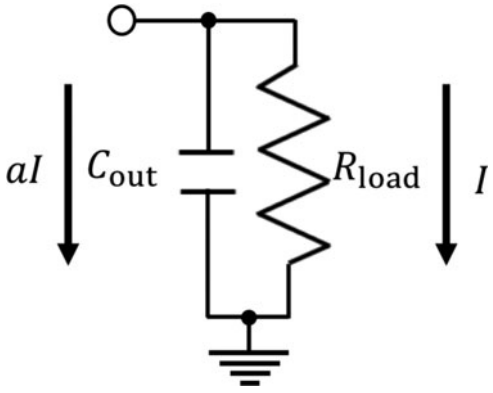

Fig. 9. Rectifier load.

Equation (22) is derived from equation (21):

$$P_{DC} = \frac{\overline{V_{out}}^2}{R_{load}} = \eta_{RF} P_{input}. \quad (22)$$

Equation (23) follows from the above equations:

$$\eta_{DC} = \eta_{RF}. \quad (23)$$

Equation (23) shows that the RF-DC conversion efficiency with CW having P_{input}/D can be obtained. In addition, equation (20) states that the optimum load of this condition becomes $1/D$ times that under the CW drive conditions. These equations are obtained with satisfied conditions of equation (12) and our theory is not related to the matching network and the value of R_{load}. Therefore, these equations are generally obtained when using pulse-modulated input and equation (12) is satisfied. Therefore, the optimum matching network is same as CW input rectifiers with DR_{load}.

III. BASIC ANALYSIS OF RF-DC CONVERSION WITH PULSE MODULATION

The rectifier with CW, which has 10 mW of input power and a 2.45 GHz frequency drive, is designed using the harmonic balance simulation. The parameters shown in Table 2 are used for the board parameter setting. Figure 4 presents a schematic of the designed single-shunt rectifier.

A) Estimation of the rectifier operation

The pulse-modulated waves have two basic frequencies: repetition and carrier frequencies. This study exploits the carrier frequency of 2.45 GHz and the repetition frequency is below 1 MHz. Thus, the pulse-modulated waves possess excessive frequency components. In this case, the rectifier operation cannot be analyzed using the harmonic balance method. Therefore, only the transient simulation is useful for analyzing the operation of rectifiers with the pulse-modulated input. However, for the transient analysis, the transient simulation requires the time step to be sufficiently small compared to the period of the carrier wave. Hence, analyzing the operation of the rectifiers by taking into account only one condition is time consuming. For this reason, the output voltage waveform is estimated using equations (13) and (14) using $f_{rising}(t)$ and $f_{falling}(t)$. The exponential function approximates the output voltage wave. It is estimated that $f_{rising}(t)$ and $f_{falling}(t)$ can be expressed by equations (15) and (16), respectively. Then, the simulation result should confirm consistency of this assumption. The output voltage of the rectifiers with a single-shot CW input is simulated. The chosen simulation parameters are the input duration, the average power, and the frequency being equal to 250 μs, 1 mW, and 2.45 GHz, respectively; R_{load} and C_{out} are 2 kΩ and 47 nF, respectively. The green line in Fig. 10 shows the simulation result of the transient. Equations (15) and (16) fit the green line using the Levenberg–Marquardt method [18]. The red and blue lines in Fig. 10 show the fitting result of equations (15) and (16), respectively. Figure 10 exhibits a complete match of the green, red, and blue lines. Therefore, the former estimation is quite correct. The application of the fitting procedure allows us to deduce the value of τ_{rising} as 3.576×10^{-5} and that of $\tau_{falling}$ as 9.408×10^{-5}. In this case, the rise and fall times become 78.6 and 206.7 μs, respectively.

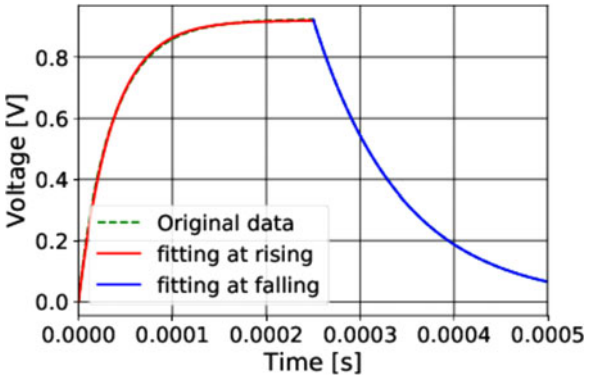

Fig. 10. Simulated V_{out} using transient analysis.

B) Estimated and simulation characteristics of the rectifiers

In this subsection, the output voltage is estimated in a steady state using the values of τ_{rising} and $\tau_{falling}$ in subsection A). Using this estimation, the V_{out} values in various conditions derived using numerical calculations are known as long as the load components are fixed. Since numerical calculations are quick, the time for analyzing the operation of rectifiers under the pulse-modulated input is reduced. If the value of E is known, the performances of rectifiers can be calculated by equations (13) and (14) using numerical analysis. E is equal to the output voltage of the rectifiers with a CW input black, which has the same power as a career wave (P_{RF}). Thus, E is calculated using the harmonic balance or transient simulations. Table 3 shows the simulated DC voltage in a steady state with the condition that the values of R_{load} and C_{out} are 2 kΩ and 47 nF, respectively. Using the data in Table 3, η_{DC}, η_{out}, and M are calculated at P_{input} of 1 mW. Figures 11, 12, and 13 show η_{out}, η_{DC}, and M, respectively; they demonstrate a good agreement between the estimation

Table 2. Board parameters of microstrip substrate in the simulations.

Description	Value
Substrate thickness	0.8 mm
Relative dielectric constant	2.53
Dielectric loss tangent	0.0018
Relative permeability	1
Conductor thickness	18 μm
Conductor conductivity	4.8×10^7 S/m

Table 3. Simulated DC voltage in the steady state.

Input power (mW)	DC voltage (V)
1.11	0.976
1.43	1.150
2.00	1.407
3.33	1.913
10.00	3.094

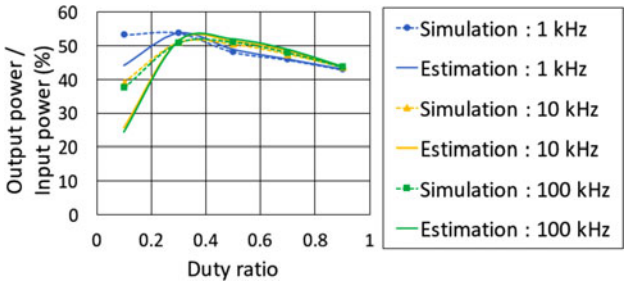

Fig. 11. Simulated and estimated η_{out} depending on f_r and D.

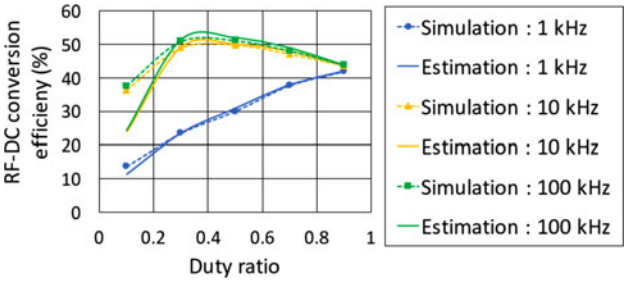

Fig. 12. Simulated and estimated η_{DC} depending on f_r and D.

and simulation results. But with $D = 0.1$, Figs 11 and 12 show differences and Fig. 13 shows a complete match. These results indicate that our proposed method is not good for estimating η_{out} and η_{DC} under a condition in which the output voltage has little fluctuation and D is also little. When D is very small, the error of the rising waveform will affect the calculation results. Figures 11 and 12 show an error of 20%. This large error can occur from only a few percent errors in the rising waveform. In addition, the transient simulation can easily generate a numerical error with small D. Therefore, the simulation and our proposed estimation method are not good for analyzing the steady state with too small D. Hence, when D is not so small and f_r is less than or equal to 100 kHz, the estimation method mentioned in subsection A) is consistent with the simulation of rectifiers under a pulse-modulated wave input.

C) Experimental characteristics of rectifiers

Figure 14 presents a rectifier fabricated using the parameters in Fig. 4. Figure 15 shows the change of η_{DC} with CW depending on P_{input} and R_{load}. In the experiments and simulations, C_{in} and C_{out} are set as 100 pF and 47 nF, respectively. The results of the experiments and simulations show similar tendencies. The rectifier experiments used the conditions shown in Table 4. Figures 16, 17, and 18 exemplify the experimental and estimation results indicating a good agreement. But, with $D = 0.1$, Figs 16 and 17 show around 10% errors. Also the experimented and simulated values (Figs. 11 and 12) have around 10% errors. These errors occur by the reasons mentioned in the previous section. Figure 16 reveals that η_{out} increases with the decrease of f_r at low D. When f_r is high, equation (12) is satisfied. In this case, the observed load resistance of rectifiers becomes $1/D$ times R_{load} because of equation (20). Letting the apparent resistance $R_{eq} = R/D$, the rectifiers operate with P_{RF} of input power and R_{eq} of load resistance. Figure 15 shows that a 20 kΩ load resistance is much higher than the optimum resistance, and the RF-DC conversion efficiency is very low under such conditions. In contrast, if equation (12) is not satisfied, and the output voltage wave becomes a pulse wave with a low f_r, the rectifier operates with P_{input}/D and 2 kΩ of input power and load resistance, respectively. A 2 kΩ load impedance is around the optimum value with from 1 to 10 mW input. Therefore, the lower D is, the more η_{output} become.

Figure 17 shows the increase in the experimental η_{DC} and the simulated η_{DC} depending on f_r. η_{DC} is proportional to D with a low f_r, when equation (12) is not satisfied, and the output voltage becomes a pulse wave. Equation (24) in this case provides the relation between η_{DC} and η_{out}:

$$\eta_{DC} = D\eta_{out}. \tag{24}$$

Thus, η_{DC} is proportional to D, consistent with the results in Fig. 17. On the other hand, Fig. 17 shows the peak around $D = 0.4$ with f_r is 10 or 100 kHz. In these cases, f_r is sufficiently high and the output voltage has little fluctuation. The apparent power and impedance are P_{input}/D and DR_L, respectively. Figure 15 shows the optimum impedance of our experimented rectifier was more than ~1 kΩ when the input power was lower than or equal to 10 mW. In this paper, D is larger than or equal to 0.1. Therefore, as D becomes smaller, the apparent input power further closer to the optimum power and the apparent resistance becomes further away from the optimum impedance. For this trade-off relationship between the apparent power and impedance, our experimented rectifier had the optimum value of D around 0.4.

Figure 18 shows the monotonic decrease of M depending on the increase of f_r and D. V_{DC} increases depending on D

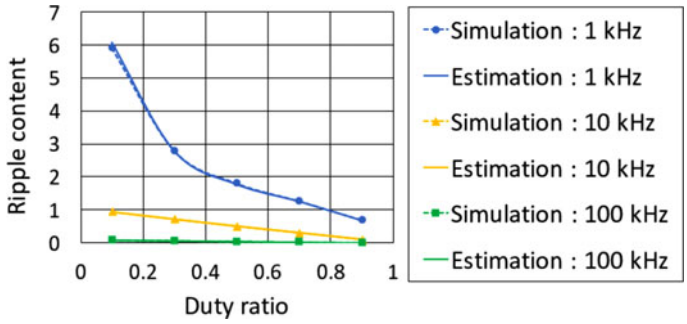

Fig. 13. Simulated and estimated M depending on f_r and D.

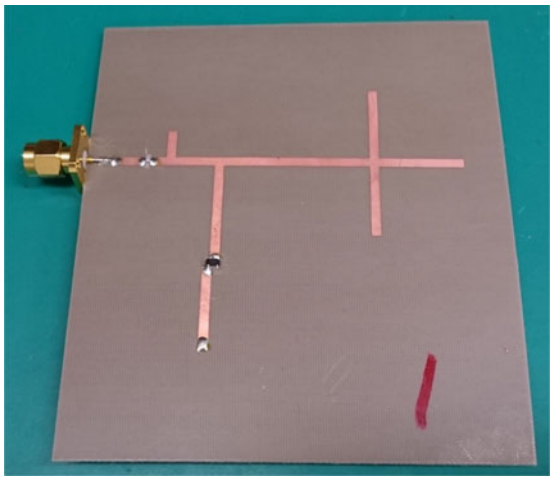

Fig. 14. An experimented rectifier.

Table 4. Parameters in the experiments in Section III subsection C).

Fixed parameters	**Value**
P_{input}	1 mW
C_{out}	47 nF
R_{load}	2 kΩ
Variable parameters	Value
f_r	From 100 Hz to 100 kHz
D	From 0.1 to 0.9

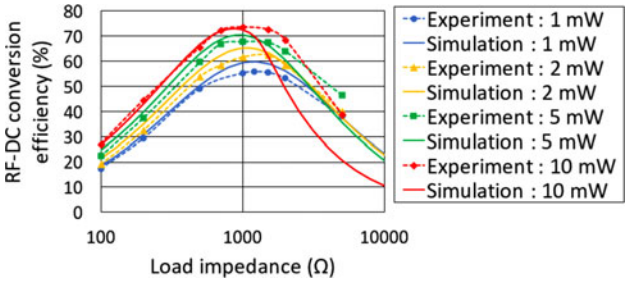

Fig. 15. The change of η_{DC} with CW input depending on P_{input} and R_{load}.

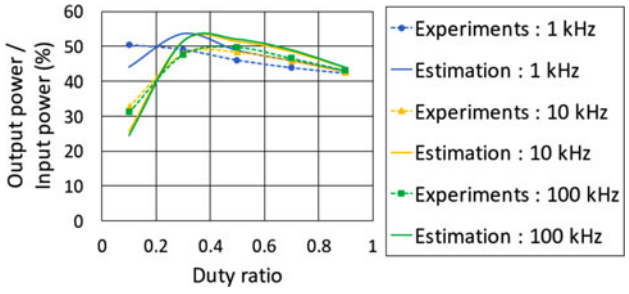

Fig. 16. Experimental and estimated η_{out} depending on f_r and D.

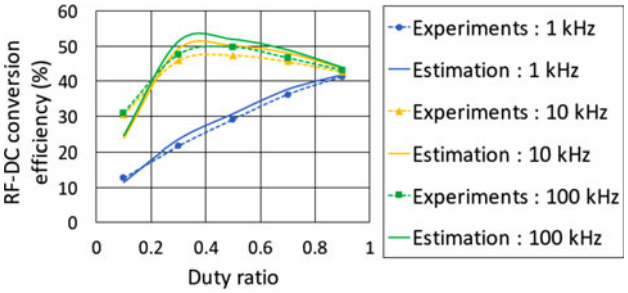

Fig. 17. Experimental and estimated η_{DC} depending on f_r and D.

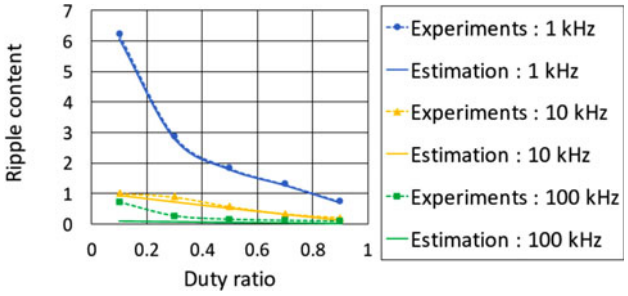

Fig. 18. Experimental and estimated M depending on f_r and D.

and max (V_{out}) − min (V_{out}) decreases depending on f_r, which explains the decrease of M in Fig. 18.

IV IMPROVEMENT OF RF-DC CONVERSION WITH PULSE MODULATION

Although simulations of the rectifiers under the pulse-modulated input are time-consuming, particularly if C_{out} is very large, V_{out} can be quickly obtained in the experiments. In this section, the operation of the rectifiers is experimentally analyzed in detail, and the results are compared in light of the theoretical discussion that was presented in Section II.

A) Influences of C_{out} on the rectifier operation

In this subsection, the validity of the condition expressed in equation (12) is examined. The parameter settings and conditions from Table 5 are used in the experiments with the outcome presented in Figs. 19, 20, and 21. In this case, $C_{out} \gg (1 - D) \times 10^{-6}$ is necessary for satisfying equation (12). Large changes occur at around C_{out} when it is equal to (1 −

Table 5. Parameters setting in Section IV subsection A).

Fixed parameters	**Value**
P_{input}	1 mW
R_{load}	1 kΩ
f_r	1 kHz
Variable parameters	Value
C_{out}	from 10 nF to 100 μF
D	0.1 or 0.5

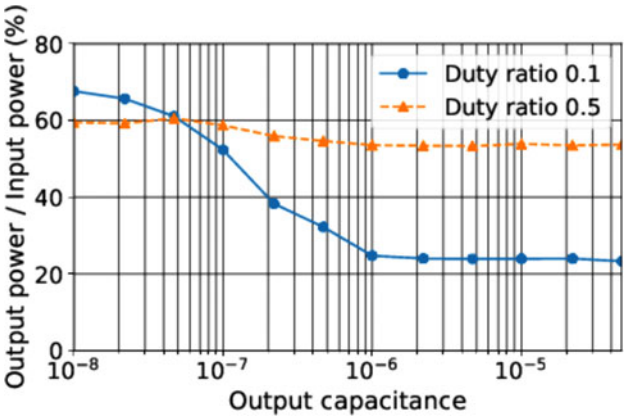

Fig. 19. Changes in η_{out} depending on C_{out} and D.

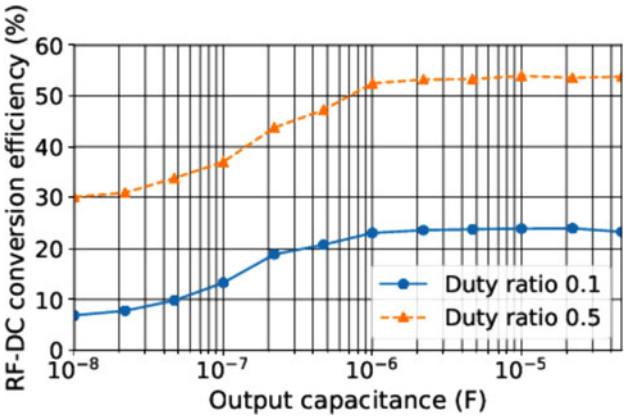

Fig. 20. Changes in η_{DC} depending on C_{out} and D.

$D) \times 10^{-6}$ as shown in Figs. 19, 20, and 21. This indicates that the condition in equation (12) is consistent with the actual operation of the rectifiers under the pulse-modulated input.

When C_{out} is sufficiently small, the output voltage becomes a pulse wave and the rectifier operates with the P_{RF} of input power and R_{load} of load resistance. Also, η_{DC} is expressed by equation (24) and η_{out} is same as that of CW input. From Fig. 15, η_{out} with $D = 0.1$ and $D = 0.5$ should be ~70 and 60% respectively, and η_{DC} with $D = 0.1$ and $D = 0.5$ should be ~7 and 30%, respectively. This assumption is consistent

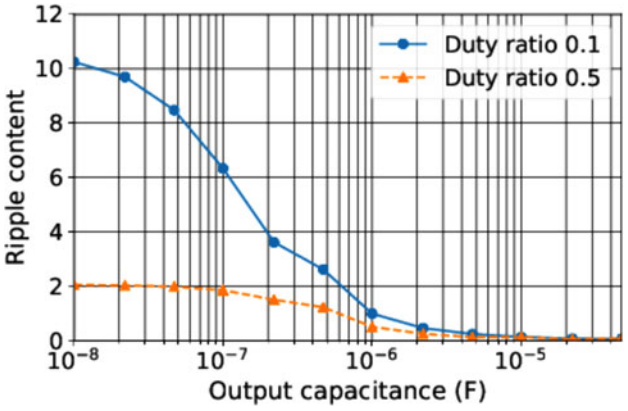

Fig. 21. Changes in M depending on C_{out} and D.

Table 6. Parameters setting in Section IV subsection B).

Fixed parameters	Value
P_{input}	1 mW
C_{out}	100 μF
f_r	1 kHz
Variable parameters	Value
R_{load}	From 100 Ω to 50 kΩ
D	0.1, 0.3, or 0.5

with Figs 19 and 20. Next, we consider the condition that C_{out} is sufficiently large. η_{out} and η_{DC} should be the same value and equal to the η_{DC} with P_{RF} of input power and R_{eq} of load resistance. This assumption is also consistent with Figs 19 and 20. These results indicate that the rectifier operation is changed by the value of C_{out}. This is the reason for the crossing in Fig. 19. If the application can use the pulse wave, the condition, where equation (12) is not satisfied, is better than satisfying equation (12). Therefore, we should change the conditions depending on applications for improving the RF-DC conversion efficiency. Figures 19 and 20 show that the C_{out} value is useful and important for managing conditions. Even if f_r is not so high, large C_{out} satisfies the conditions of equation (12). Therefore, pulse modulation is useful for all applications by managing the C_{out} value.

B) Improvement in η_{DC} with a sufficiently large smoothing capacitor

In this subsection, the η_{DC} is discussed depending on the R_{load}, which satisfies the condition of equation (12). The parameters shown in Table 6 are used in the experiments. A 100 μF C_{out} is sufficiently large for satisfying the condition of equation (12), wherein V_{out} is regarded as a constant. Figure 22 reveals the change of η_{DC} depending on R_{load} and D and the increasing maximum η_{DC} at the vanishing D, in accordance with equation (23). Figure 23 shows the comparison between the η_{DC} with the pulse-modulated-input (a duty ratio of 0.5 and an input power of 1 mW) and that with CW input power of 2 mW. The green line indicates the relation of the RF-DC conversion efficiency with the CW, which is 2 mW versus $1/D$ times R_{load}. Figure 24 shows the comparison between the η_{DC} under the pulse-modulated input (a duty ratio of 0.1 and an input power of 1 mW) and that with CW input of 10 mW input power. The green line indicates the relation of the RF-DC conversion efficiency with the CW, which is

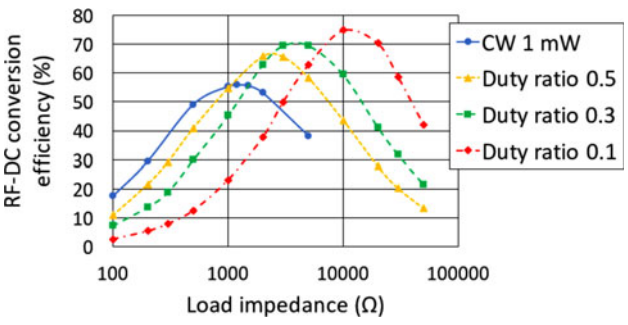

Fig. 22. The change in the η_{DC} depends on the R_{load} with sufficiently large C_{out}.

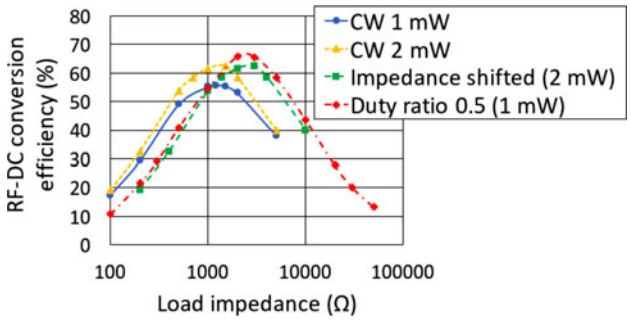

Fig. 23. The comparison between the η_{DC} with pulse-modulated input, which has the duty ratio of 0.5 and the input power of 1 mW, and that with CW input, which has the input power of 2 mW.

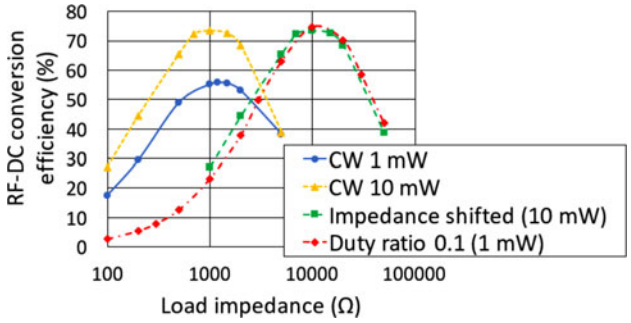

Fig. 24. The comparison between the η_{DC} with pulse-modulated input, which has the duty ratio of 0.1 and the input power of 1 mW, and that with CW input, which has the input power of 10 mW.

10 mW versus $1/D$ times R_{load}. The red and green lines match as shown in Figs 23 and 24, respectively. This is consistent with equations (20) and (23) and proves that by using pulse modulation, the RF-DC conversion efficiency with CW, which has P_{input}/D and the optimum resistance shift $1/D$ times R_{load}, can be obtained. This indicates that the RF-DC conversion efficiency of the rectifiers having a lower input can be improved using pulse modulation.

V. CONCLUSIONS

In this study, the operation of the rectifiers under the pulse-modulated input has been discussed. The fluctuation of the output voltage wave has to be considered when using the pulse-modulated waves. This paper shows the estimation, simulation, and experimentation of rectifiers under the pulse-modulated input, and all of the results are in good agreement.

A smoothing capacitance C_{out} is quite important for the improvement of RF-DC conversion efficiency that can be attained by using a pulse modulation. When the capacitance is sufficiently small, the output voltage wave is almost a pulse wave and its η_{DC} is not so high. Conversely, with a sufficiently large capacitance, η_{DC} is improved from η_{RF} with P_{input} to η_{RF} with P_{RF}. The necessary condition for the smoothing capacitance value was discussed in Section II subsection B) and is expressed by equation (12). The optimum impedance with equation (12) satisfied was also discussed in Section II subsection C) and that is increased to an inverse of the duty ratio times η_{RF} with P_{RF} input.

We proposed the estimation method of a rectifier operation under a pulse-modulated wave input and the consistency with simulation results was discussed in Section III subsections A) and B). In addition, we compared the estimation and experimental results in Section III subsection C). When $D = 0.1$, the estimation and simulation results are not matched and the reason seems to be the calculation error. However, at least when D is larger than or equal to 0.3, our proposed method shows good consistency with both simulation and experimental results. In addition, our proposed method takes less time than the transient simulation. Therefore, this method was effective for estimating the rectifier operations with not so high f_t.

The experiments regarding the influence of the smoothing capacitor and the effectiveness of a pulse modulation are discussed in Section IV. The condition of equation (12) was consistent with the experimental result. The maximum RF-DC conversion efficiency was improved by using pulse modulation. The characteristics were also consistent with the discussion in Section II. C_{out} value is important and useful for managing the conditions and it decides whether equation (12) is satisfied or not. Therefore, even if f_r is not too high, pulse modulation is useful with using a proper smoothing capacitance.

Consequently, we showed the effectiveness of a pulse modulation and succeeded in performing the operational analysis of the rectifiers with a pulse-modulated input.

REFERENCES

[1] Brown, W.: Experiments in the transportation of energy by microwave beam. In IRE International Convention Record, IEEE, **12**, 1966, 8–17.

[2] Brown, W.C.: The history of power transmission by radio waves. *IEEE Trans. Microwave Theory Technol.*, **32** (9) (1984), 1230–1242.

[3] Shinohara, N.: Simultaneous WPT and wireless communication with TDD algorithm at same frequency band. In Georgiadis, A.; Nikoletseas, S.; Yang, Y.: editor, Wireless Power Transfer Algorithms, Technologies and Applications in Ad Hoc Communication Networks, chapter 9, Springer, 7 2016, 211–230.

[4] Claessens, S.; Schreurs, D.; Pollin, S.: SWIPT with biased ask modulation and dual-purpose hardware. In *Wireless Power Transfer Conference (WPTC)*, 2017 IEEE, IEEE, 2017, 1–4.

[5] Claessens, S.; Pan, N.; Rajabi, M.; Schreurs, D.; Pollin, S.: Enhanced biased ask modulation performance for SWIPT with AWGN channel and dual-purpose hardware. *IEEE Trans. Microwave Theory Technol.*, **66** (2018), 3478–3486.

[6] Matsumoto, H.; Takei, K.: An experimental study of passive uhf RFID system with longer communication range. In *Microwave Conference, 2007*. APMC 2007. Asia-Pacific, IEEE, 2007, 1–4.

[7] Nahas, J.J.: Modeling and computer simulation of a microwave-to-dc energy conversion element. *IEEE Trans. Microwave Theory Technol.*, **23** (12) (1975), 1030–1035.

[8] Boyakhchyan, G.P.; Vanke, V.; Lesota, S.K.; Maslovskiy, F.N.; Novitskiy, V.A.: Analytical calculation of a high-efficiency microwave rectifier employing a Schottky-barrier diode. *Telecommun. Radio Eng.*, **37** (10) (1983), 64–66.

[9] Guo, J.; Zhang, H.; Zhu, X.: Theoretical analysis of RF-DC conversion efficiency for class-f rectifiers. IEEE Trans. *Microwave Theory Technol.*, **62** (4) (2014), 977–985.

[10] McSpadden, J.O.; Fan, L.; Chang, K.: Design and experiments of a high-conversion-efficiency 5.8-GHz rectenna. *IEEE Trans. Microwave Theory Technol.*, **46** (12) (1998), 2053–2060.

[11] Yoo, T.-W.; Chang, K.: Theoretical and experimental development of 10 and 35 GHz rectennas. *IEEE Trans. Microwave Theory Technol.*, **40** (6) (1992), 1259–1266.

[12] Boaventura, A.; Belo, D.; Fernandes, R.; Collado, A.; Georgiadis, A.; Carvalho, N.B.: Boosting the efficiency: unconventional waveform design for efficient wireless power transfer. *IEEE Microwave Mag.*, **16** (3) (2015), 87–96.

[13] Collado, A.; Georgiadis, A.: Improving wireless power transmission efficiency using chaotic waveforms. In *Microwave Symposium Digest (MTT)*, 2012 IEEE MTT-S International, IEEE, 2012, 1–3.

[14] Lo, C.-C.; Yang, Y.-L.; Tsai, C.-L.; Lee, C.-S.; Yang, C.-L.: Novel wireless impulsive power transmission to enhance the conversion efficiency for low input power. In *Microwave Workshop Series on Innovative Wireless Power Transmission: Technologies, Systems, and Applications (IMWS), 2011 IEEE MTT-S International*, IEEE, 2011, 55–58.

[15] Carvalho, N.B.; Remley, K.A.; Schreurs, D.; Card, K.G.: Multisine signals for wireless system test and design [application notes]. *IEEE Microwave Mag.*, **9** (3) (2008), 122–138.

[16] Collado, A.; Georgiadis, A.: Optimal waveforms for efficient wireless power transmission. *IEEE Microwave Compon. Lett.*, **24** (5) (2014), 354–356.

[17] Ibrahim, R. et al.: Novel design for a rectenna to collect pulse waves at 2.4 GHz. *IEEE Trans. Microwave Theory Technol.*, **66** (1) (2018), 357–365.

[18] Moré, J.J.: The Levenberg–Marquardt algorithm: implementation and theory. In *Numerical Analysis*, Springer, 1978, 105–116.

Takashi Hirakawa received his B.S. degree in Electrical and Electronic Engineering from Kyoto University in 2016. From 2016, he is studying about microwave techniques in the Electrical Engineering of Kyoto University.

Ce Wang received his B.S. degree in Integrated System Engineering from the Kyushu Institute of Technology, Fukuoka, Japan, in 2014. He is currently pursuing his M.S. degree in electrical engineering at Kyoto University. His current research interests include low-power rectenna and wireless power transmission system design.

Naoki Shinohara received his B.E. degree in electronic engineering, M.E. and Ph.D. (Eng.) degrees in electrical engineering from Kyoto University, Japan, in 1991, 1993, and 1996, respectively. He was a research associate in Kyoto University from 1996. From 2010, he has been a professor in Kyoto University. He has been engaged in research on Solar Power Station/Satellite and Microwave Power Transmission system. He is IEEE MTT-S Technical Committee 26 (Wireless Power Transfer and Conversion) vice chair, IEEE MTT-S Kansai Chapter TPC member, IEEE Wireless Power Transfer Conference advisory committee member, executive editor of international journal Wireless Power Transfer (Cambridge Press), technical committee on IEICE Wireless Power Transfer, communications society member, Japan Society of Electromagnetic Wave Energy Applications vice president, Space Solar Power Systems Society board member, Wireless Power Transfer Consortium for Practical Applications (WiPoT) chair, and Wireless Power Management Consortium (WPMc) chair.